Original Article | Neurointervention

eISSN 2005-8330
https://doi.org/10.3348/kjr.2021.0332
Korean J Radiol 2022;23(2):246-255

Korean Journal of Radiology
KJR

Usefulness of Silent MRA for Evaluation of Aneurysm after Stent-Assisted Coil Embolization

You Na Kim[1], Jin Wook Choi[1], Yong Cheol Lim[2], Jihye Song[2], Ji Hyun Park[3], Woo Sang Jung[1, 4]

Departments of [1]Radiology and [2]Neurosurgery, Ajou University School of Medicine, Ajou University Medical Center, Suwon, Korea; [3]Office of Biostatistics, Medical Research Collaborating Center, Ajou Research Institute for Innovative Medicine, Ajou University Medical Center, Suwon, Korea; [4]Department of Radiology, Kangwon National University College of Medicine, Chuncheon, Korea

Objective: To determine the usefulness of Silent MR angiography (MRA) for evaluating intracranial aneurysms treated with stent-assisted coil embolization.

Materials and Methods: Ninety-nine patients (101 aneurysms) treated with stent-assisted coil embolization (Neuroform atlas, 71 cases; Enterprise, 17; LVIS Jr, 9; and Solitaire AB, 4 cases) underwent time-of-flight (TOF) MRA and Silent MRA in the same session using a 3T MRI system within 24 hours of embolization. Two radiologists independently interpreted both MRA images retrospectively and rated the image quality using a 5-point Likert scale. The image quality and diagnostic accuracy of the two modalities in the detection of aneurysm occlusion were further compared based on the stent design and the site of aneurysm.

Results: The average image quality scores of the Silent MRA and TOF MRA were 4.38 ± 0.83 and 2.78 ± 1.04, respectively (p < 0.001), with an almost perfect interobserver agreement. Silent MRA had a significantly higher image quality score than TOF MRA at the distal internal carotid artery (n = 57, 4.25 ± 0.91 vs. 3.05 ± 1.16, p < 0.001), middle cerebral artery (n = 21, 4.57 ± 0.75 vs. 2.19 ± 0.68, p < 0.001), anterior cerebral artery (n = 13, 4.54 ± 0.66 vs. 2.46 ± 0.66, p < 0.001), and posterior circulation artery (n = 10, 4.50 ± 0.71 vs. 2.90 ± 0.74, p = 0.013). Silent MRA had superior image quality score to TOF MRA in the stented arteries when using Neuroform atlas (4.66 ± 0.53 vs. 3.21 ± 0.84, p < 0.001), Enterprise (3.29 ± 1.59 vs. 1.59 ± 0.51, p = 0.003), LVIS Jr (4.33 ± 1.89 vs. 1.89 ± 0.78, p = 0.033), and Solitaire AB stents (4.00 ± 2.25 vs. 2.25 ± 0.96, p = 0.356). The interpretation of the status of aneurysm occlusion exhibited significantly higher sensitivity with Silent MRA than with TOF MRA when using the Neuroform Atlas stent (96.4% vs. 14.3%, respectively, p < 0.001) and LVIS Jr stent (100% vs. 20%, respectively, p = 0.046).

Conclusion: Silent MRA can be useful to evaluate aneurysms treated with stent-assisted coil embolization, regardless of the aneurysm location and type of stent used.

Keywords: *Silent magnetic resonance angiography; Time-of-flight MRA; Stent-assisted coil embolization; Stent design; Zero TE MRA*

INTRODUCTION

Endovascular treatment for intracranial aneurysms has been widely used since the International Subarachnoid Aneurysm Trial [1]. The number of cases of coil embolization for aneurysms is increasing; the stent-assisted technique has a wider application because it can be employed in cases that are difficult to treat with conventional coil embolization [2]. Nevertheless, there is still a risk of aneurysm recurrence with stent-assisted coil embolization due to coil compaction. Therefore, treated intracranial aneurysms require follow-up imaging to evaluate the occlusion status of the aneurysm.

Time-of-flight MR angiography (TOF MRA) is widely used as a noninvasive substitute for digital subtraction angiography (DSA) for the follow-up of conventional coil embolization [3,4]. However, the visualization of the flow of the treated site and the occlusion status in patients

Received: April 22, 2021 **Revised:** August 20, 2021
Accepted: August 22, 2021
Corresponding author: Woo Sang Jung, MD, Department of Radiology, Ajou University School of Medicine, Ajou University Medical Center, 164 World cup-ro, Yeongtong-gu, Suwon 16499, Korea.
• E-mail: stepws@naver.com

Korean Journal of Radiology
KJR

undergoing stent-assisted coil embolization are limited because of magnetic susceptibility artifacts [3,4]. In clinical practice, DSA is a well-known gold standard modality for the follow-up of treated aneurysms because of its high spatial resolution, three-dimensional (3D) imaging, and dynamic information [5]. However, DSA is an invasive procedure with disadvantages such as unavoidable radiation exposure, contrast material-induced complications, hematoma at the puncture site, and risk of neurological complications due to thromboembolism or arterial dissection [6]. Therefore, noninvasive imaging techniques are frequently preferred because procedure-related risks may accumulate when procedures are repeated over the follow-up period [5]. In previous studies, non-contrast-enhanced (CE) MRA using the Silent Scan algorithm (Silent MRA) or pointwise encoding time reduction with radial acquisition with subtraction-based MRA has been introduced as an imaging modality for the follow-up of treated intracranial aneurysms that can overcome the disadvantages of TOF MRA [7-13].

Over the past few years, variable intracranial stents, including the Neuroform atlas [14,15] (Stryker), Enterprise [16,17] (Codman), LVIS Jr [18-20] (MicroVention), Solitaire AB [21,22] (eV3) have been implemented for stent-assisted coil embolization of wide-necked aneurysms. Nonetheless, existing studies on the usefulness of Silent MRA for evaluating treated aneurysms have limited generalizability, since only a small number of stent types were included.

We hypothesized that Silent MRA could be a first-line, noninvasive imaging modality for the follow-up of aneurysms treated with stent-assisted coil embolization, regardless of the aneurysm location or stent type. Therefore, this study aimed to investigate the clinical usefulness of Silent MRA in evaluating the image quality and diagnostic accuracy of treated intracranial aneurysms in diverse arterial locations and with multiple stent types, when compared with TOF MRA.

MATERIALS AND METHODS

Ethical Approval

Ethical approval was obtained from the relevant Institutional Review Board. The requirement for written informed consent was waived because of the retrospective nature of this study (IRB No. MED-MDB-20-508).

Patient and Aneurysm Characteristics

Between November 2019 and December 2020, 103 aneurysms in 101 patients treated with stent-assisted coil embolization were retrospectively examined. Two patients were excluded from the study because of poor MRA image quality. The remaining 99 patients with 101 aneurysms comprised 27 male and 72 female with a mean age of 57.9 ± 10.3 years (range, 18–78 years). The aneurysms in these 99 patients were located in the distal internal carotid artery (57/101, 56.4%), middle cerebral artery (21/101, 20.8%), anterior cerebral artery (13/101, 12.9%), and posterior circulation artery (10/101, 9.9%). The stents used to treat the aneurysm were the Neuroform Atlas stent (71/101, 70.3%), Enterprise stent (17/101, 16.8%), LVIS Jr stent (9/101, 8.9%), and Solitaire AB stent (4/101, 4.0%).

All patients were followed up using TOF MRA and Silent MRA performed in the same session within 24 hours of embolization. The image quality of the stented arterial segment and diagnostic performance of the treated aneurysm were compared with follow-up MRA images, based on the final DSA images obtained during the stent-assisted coil embolization procedure, used as a reference standard.

MRA Scan Parameters

Silent MRA and TOF MRA were performed with 3T MRA (Discovery™ MR750w; GE Healthcare) with a 24-channel head coil. The scan parameters of Silent MRA were as follows: repetition time (TR), 1096 ms; echo time (TE), 0.016 ms; flip angle, 5°; field of view (FOV), 200 x 200 mm; matrix, 180 x 180; bandwidth, ± 25 kHz; section thickness, 1.2 mm; number of excitations (NEX), 1.6; and acquisition time, 7 minutes and 43 seconds. The scan parameters of 3D TOF MRA were as follows: TR, 19 ms; TE, 3.0 ms; flip angle, 15°; FOV, 117 x 150 mm; matrix, 512 x 300; bandwidth, ± 50 kHz; section thickness, 1.2 mm; NEX, 0.85; and acquisition time, 5 minutes, 47 seconds (Table 1).

Table 1. Scan Parameters of Silent MRA and TOF MRA

Parameter	Silent MRA	TOF MRA
FOV, mm^2	200 x 200	117 x 150
Acquisition Matrix	180 x 180	512 x 300
TR/TE, ms	1096/0.016	19/3.0
Flip angle, °	5	15
Bandwidth, kHz	25	50
Slice thickness, mm	1.2	1.2
NEX	1.60	0.85
Acquisition time, minutes:seconds	7:43	5:47

FOV = field of view, MRA = MR angiography, NEX = number of excitations, Silent MRA = MRA using the Silent Scan algorithm, TE = echo time, TOF = time-of-flight, TR = repetition time

https://doi.org/10.3348/kjr.2021.0332

Image Analysis

All DSA, Silent MRA, and 3D TOF MRA series scans were anonymized by random number assignment. The two types of MRA images were assessed separately to minimize bias due to knowledge of the results of the other MRA images. We used both maximum intensity projection and source images. All images were independently evaluated in random order by two radiologists (who had 6 and 3 years of experience in neuroradiology, respectively) on a picture archiving and communication system. In all images, the window width and window level can be modified for evaluation. The locations of the treated aneurysms were provided to the two observers because pretreatment DSA images were unavailable.

The image quality for visualization of the stented artery was assessed based on a 5-point Likert scale as follows: 1) not visible (almost no signal); 2) poor (structures are slightly visible but with substantial blurring or artifacts); 3) acceptable (diagnostic information of acceptable quality with medium blurring or artifacts); 4) good (diagnostic information of good quality with minimal blurring or artifacts); and 5) excellent (diagnostic information of good quality without blurring or artifacts) [9]. In addition, the occlusion status of the stented aneurysm was evaluated using a dual rating system (total occlusion/remnant). The remnant aneurysm included Raymond-Roy class II and III (residual neck or aneurysm) [23]. The aforementioned two readers evaluated the aneurysm occlusion status, using DSA as the reference standard, and performed image analysis of both Silent MRA and TOF MRA to evaluate the diagnostic accuracy of the two modalities. The two readers analyzed all cases together, using stent type, and aneurysm sites, respectively.

Statistical Analysis

Interobserver agreement in the evaluation was assessed using weighted κ statistics. According to Viera and Garrett [24], the weighted κ was interpreted as follows: < 0, less than chance agreement; 0.01–0.10, slight agreement; 0.21–0.40, fair agreement; 0.41–0.60, moderate agreement; 0.61–0.80, substantial agreement; and 0.81–0.99, almost perfect agreement. To compare the scores of the Silent MRA and TOF MRA, the scores of each image set from the two readers were averaged, and the Mann-Whitney U test was performed. To compare the diagnostic accuracy of the Silent MRA and TOF MRA in evaluating the occlusion status of stented aneurysms, sensitivity and specificity were compared using McNemar's test [25]. $p < 0.05$ was considered statistically significant.

RESULTS

Among 101 stented aneurysms with standard DSA images, 62 (61.4%) were of the complete occlusion type, and 39 (38.6%) were remnant aneurysms. The characteristics of patients and aneurysms are summarized in Table 2. The interobserver agreements were comparable between Silent MRA (κ = 0.87, $p < 0.001$) and TOF MRA (κ = 0.91, $p < 0.001$).

The mean scores for image quality were higher for Silent MRA than for TOF MRA (4.38 ± 0.83, 2.78 ± 1.04, $p < 0.001$). The assessment of the image quality of the stented aneurysm according to the aneurysm location and stent design is shown in Tables 3 and 4. All stented arterial segments showed significantly better image quality regardless of the aneurysm location on Silent MRA than that on TOF MRA, at the distal internal carotid artery (n = 57, 4.25 ± 0.91 vs. 3.05 ± 1.16, $p < 0.001$), middle cerebral artery (n = 21, 4.57 ± 0.75 vs. 2.19 ± 0.68, $p < 0.001$), anterior cerebral artery (n = 13, 4.54 ± 0.66 vs. 2.46 ± 0.66, $p < 0.001$), and posterior cerebral artery (n = 10, 4.50 ± 0.71 vs. 2.90 ± 0.74, $p = 0.013$), respectively. Moreover, the image quality of the stented segment according to the stent

Table 2. Characteristics of Patients with Aneurysms

Parameters	Values
Age, year, mean ± SD	57.9 ± 10.3
Sex, female:male	27:72
Aneurysm status (for 101 aneurysms)	
Presentation	
Ruptured	0
Unruptured	101
Location	
ICA	57
MCA	21
ACA	13
Posterior circulation	10
Occlusion result	
Complete occlusion	62
Neck remnant	39
Stent type (for 101 aneurysms)	
Neuroform Atlas	71
Enterprise	17
LVIS	9
Solitaire	4

ACA = anterior cerebral artery, ICA = internal carotid artery, MCA = middle cerebral artery, SD = standard deviation

https://doi.org/10.3348/kjr.2021.0332

Korean Journal of Radiology
KJR

type used was significantly superior on Silent MRA than on TOF-MRA, as follows: Neuroform atlas (n = 71, 4.66 ± 0.53 vs. 3.21 ± 0.84, $p < 0.001$), Enterprise (n = 17, 3.29 ± 0.85 vs. 1.59 ± 0.51, $p = 0.003$), and LVIS Jr (n = 9, 4.33 ± 1.89 vs. 1.89 ± 0.78, $p = 0.008$), respectively.

Table 5 demonstrates the subgroup analysis of the sensitivity, specificity, positive predictive value, and negative predictive value of Silent MRA and TOF MRA for evaluating the status of the aneurysm occlusion with regard to the stent type. Subgroup analysis showed significantly higher sensitivity with Silent MRA than with TOF MRA using the Neuroform Atlas (96.4% vs. 14.3%, $p < 0.001$) and LVIS Jr (100% vs. 20%, $p = 0.046$) stents.

Subgroup analysis showed that image quality was better in open-cell stents (Neuroform Atlas) than in closed-cell stents (Enterprise, LVIS Jr., Solitaire AB), regardless of Silent and TOF MRA (Supplementary Table 1). Furthermore, regardless of stent design, Silent MRA showed significantly better sensitivity than TOF MRA (Supplementary Table 2).

Figures 1-4 show representative cases for different stent designs.

Table 3. Assessment of Image Quality according to Aneurysm Location on Silent MRA and TOF MRA

Location	Silent MRA	TOF MRA	*P*
dICA (n = 57)	4.25 ± 0.91	3.05 ± 1.16	< 0.001
MCA (n = 21)	4.57 ± 0.75	2.19 ± 0.68	< 0.001
ACA (n = 13)	4.54 ± 0.66	2.46 ± 0.66	< 0.001
Posterior (n = 10)	4.50 ± 0.71	2.90 ± 0.74	0.013

Data are mean ± standard deviation. ACA = anterior cerebral artery, dICA = distal internal carotid artery, MCA = middle cerebral artery, MRA = MR angiography, Silent MRA = MRA using the Silent Scan algorithm, TOF = time-of-flight

Table 4. Assessment of Image Quality according to the Stent Design on Silent MRA and TOF MRA

Type of Stent	Silent MRA	TOF MRA	*P*
Neuroform atlas (n = 71)	4.66 ± 0.53	3.21 ± 0.84	< 0.001
Enterprise (n = 17)	3.29 ± 0.85	1.59 ± 0.51	0.003
LVIS Jr (n = 9)	4.33 ± 1.89	1.89 ± 0.78	0.008
Solitaire AB stent (n = 4)	4.00 ± 1.15	2.25 ± 0.96	0.089

Data are mean ± standard deviation. MRA = MR angiography, Silent MRA = MRA using the Silent Scan algorithm, TOF = time-of-flight

DISCUSSION

Our study demonstrated that Silent MRA offered superior image quality in visualizing stented aneurysms regardless of the aneurysm location and stent type when compared with TOF MRA. Furthermore, Silent MRA showed significantly higher diagnostic performance for evaluating aneurysm occlusion status than TOF MRA with the Neuroform atlas, Enterprise, and LVIS Jr stent designs.

Several studies have reported that Silent MRA is useful for visualizing the stented site following stent-assisted coil embolization [8-13]. Unlike previous studies, we included more arterial sites and stent types to demonstrate the usefulness of Silent MRA. Compared with TOF MRA, Silent MRA provides a higher quality view of stented arterial segments treated with the Neuroform atlas, Enterprise, and LVIS Jr stents, and aneurysms at all locations. In addition, this study measured the diagnostic performance of TOF MRA and Silent MRA in the detection of remnant aneurysms based on the different types of stents. Compared

Table 5. Diagnostic Accuracy of Silent MRA and TOF MRA for Evaluating the Status of Aneurysm Occlusion in Subgroups

Type of Stent	Type of MRA	Sensitivity (%)	Specificity (%)	PPV (%)	NPV (%)
Neuroform (n = 71)	Silent	96.4	100	100	97.7
	TOF	14.3	100	100	64.2
	p value	< 0.001	NA		
Enterprise (n = 17)	Silent	100	100	100	100
	TOF	50	100	100	86.7
	p value	0.157	NA		
LVIS Jr (n = 9)	Silent	100	100	100	100
	TOF	20	100	100	50
	p value	0.046	NA		
Solitaire AB (n = 4)	Silent	100	100	100	100
	TOF	50	100	100	66.7
	p value	0.317	NA		

MRA = MR angiography, NA = not applied, NPV = negative predictive value, PPV = positive predictive value, Silent MRA = MRA using the Silent Scan algorithm, TOF = time-of-flight

https://doi.org/10.3348/kjr.2021.0332

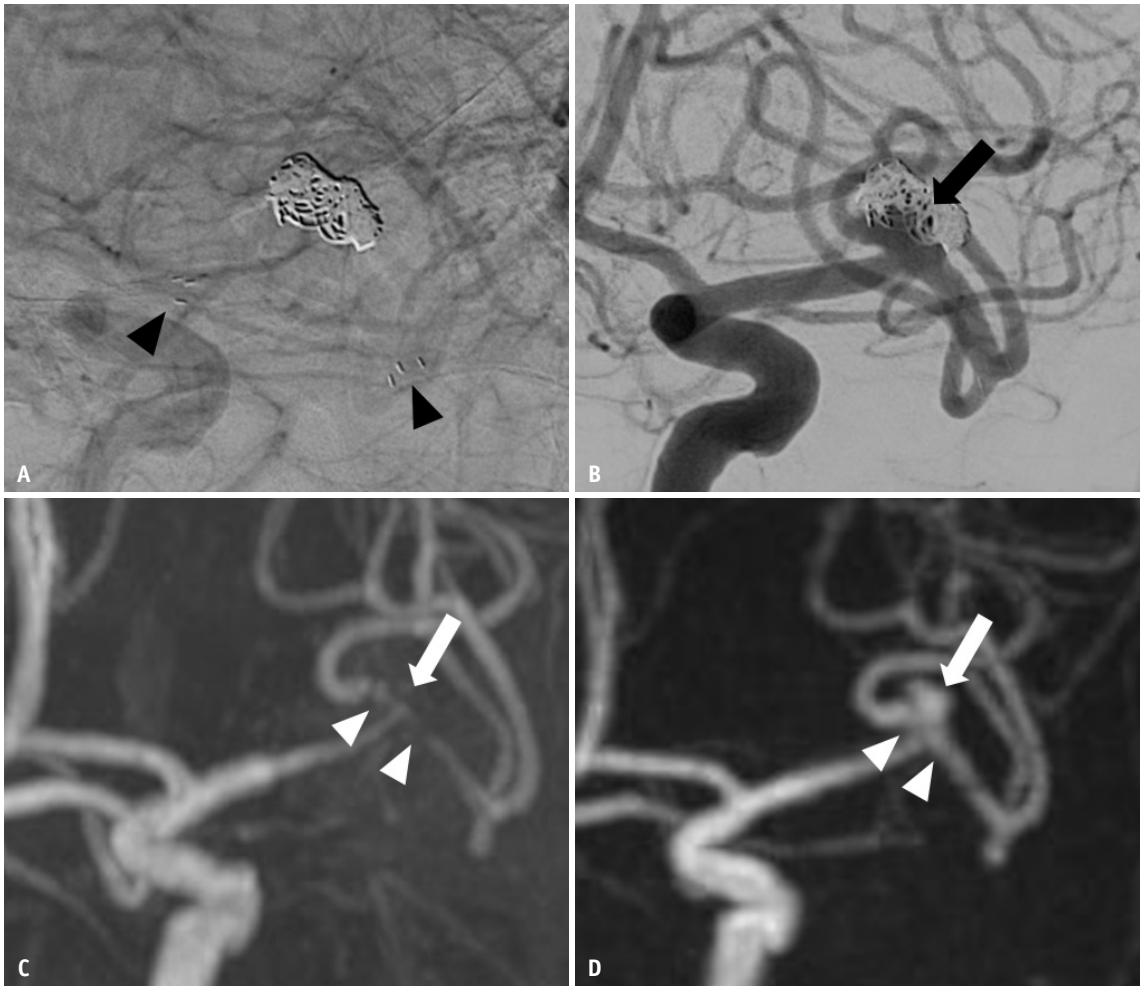

Fig. 1. Images of a 58-year-old male with a treated aneurysm in the left MCA bifurcation.
A. Stent-assisted coil embolization was performed with a Neuroform Atlas stent. Arrowheads indicate the implanted stent marker. **B.** Final angiography during the embolization procedure shows the neck remnant (arrow) of the aneurysm sac. **C.** Time-of-flight MRA shows poor visualization at the stented segment of MCA (arrowheads), and the neck remnant is not depicted (arrow). **D.** Silent MRA shows excellent visualization at the stented segment (arrowheads), and the neck remnant is fully depicted (arrow). MCA = middle cerebral artery, MRA = MR angiography

to TOF MRA, Silent MRA was better at detecting remnant aneurysms.

It is difficult to visualize the flow of stented artery on TOF MRA because of susceptibility artifacts or the radiofrequency (RF) shielding effect of intracranial stents. The RF shielding artifact is caused by eddy currents induced in the stent. These eddy currents produce an opposing RF field, which reduces the sensitivity of the receiving and emitting signals within the stent. The RF shielding artifact may be decreased by increasing the RF power of the excitation pulse [26,27].

A high-power RF pulse is required to create an excitation pulse with a high flip angle, which is proportional to the integral of the RF pulse. The higher the flip angle used, the greater the transverse magnetization created; the transverse magnetization of the unsaturated blood or fast arterial flow in the imaging plane increases [3]. Therefore, visualization of the neck remnant is difficult, even if a higher flip angle increases the signal intensity in the stent. Silent MRA imaging was performed using the Silent pulse sequence (GE Healthcare). The Silent Scan uses zero TE (ZTE), which employs a nonselective RF excitation pulse and a 3D radial center-out k-space trajectory. The imaging encoding starts immediately after the end of the RF excitation to fill the center of the k-space, which is the nominal ZTE. The RF duration should be maintained short (approximately 8–16 μs), and the flip angle is limited in ZTE to minimize the delay between the RF pulse and the transmit-receive switching time. Additionally, a limited excitation bandwidth was used to avoid disturbing the spin excitation [28]. The

https://doi.org/10.3348/kjr.2021.0332

Korean Journal of Radiology
KJR

Fig. 2. Images of a 66-year-old female with a treated aneurysm at the basilar top.
A. Stent-assisted coil embolization was performed using an Enterprise stent. Arrowheads indicate implanted stent markers. **B.** Final angiography during the embolization procedure shows the neck remnant of the aneurysm sac. **C.** Time-of-flight MRA on the same day shows complete signal loss at the stented segment (arrowhead) of the basilar artery, and the neck remnant is partially depicted (arrow). **D.** Silent MRA on the same day shows acceptable visualization of the basilar artery (arrowhead), and the neck remnant is fully depicted (arrow). MRA = MR angiography

Silent Scan includes the ZTE combined with arterial spin-labeling technique to prepare a pulse for the visualization of blood flow. In Silent MRA, the non-labeled image obtained before the labeling pulse is the control image, and the final image is reconstructed with data subtracted from the labeled image that is obtained after the labeling pulse. This ZTE can decrease magnetic susceptibility by minimizing the phase dispersion of the labeled blood flow signal in the voxel space, thereby enabling visualization of the blood flow in the stent [7].

We compared the image quality and diagnostic accuracy of the two imaging modalities with respect to the four recent representative stents used in stent-assisted coil embolization. Different stents were examined, with the assumption that the cell design and thickness of the stent struts would affect the determination of the degree of RF shielding effect and the occurrence of susceptibility artifacts. A thinner stent strut of the Neuroform Atlas stent could especially lower the incidence of susceptibility artifacts and therefore be visualized better [29,30]. The Solitaire AB stent has the thinnest stent strut, closed-cell design, and open-slit design. Owing to the open slit design, the overlap range of the stent strut was determined according to the relationship between the diameter of the stent and that of the vessel. Therefore, artifacts associated with the Solitaire stent on MRI could be easily predicted

 https://doi.org/10.3348/kjr.2021.0332

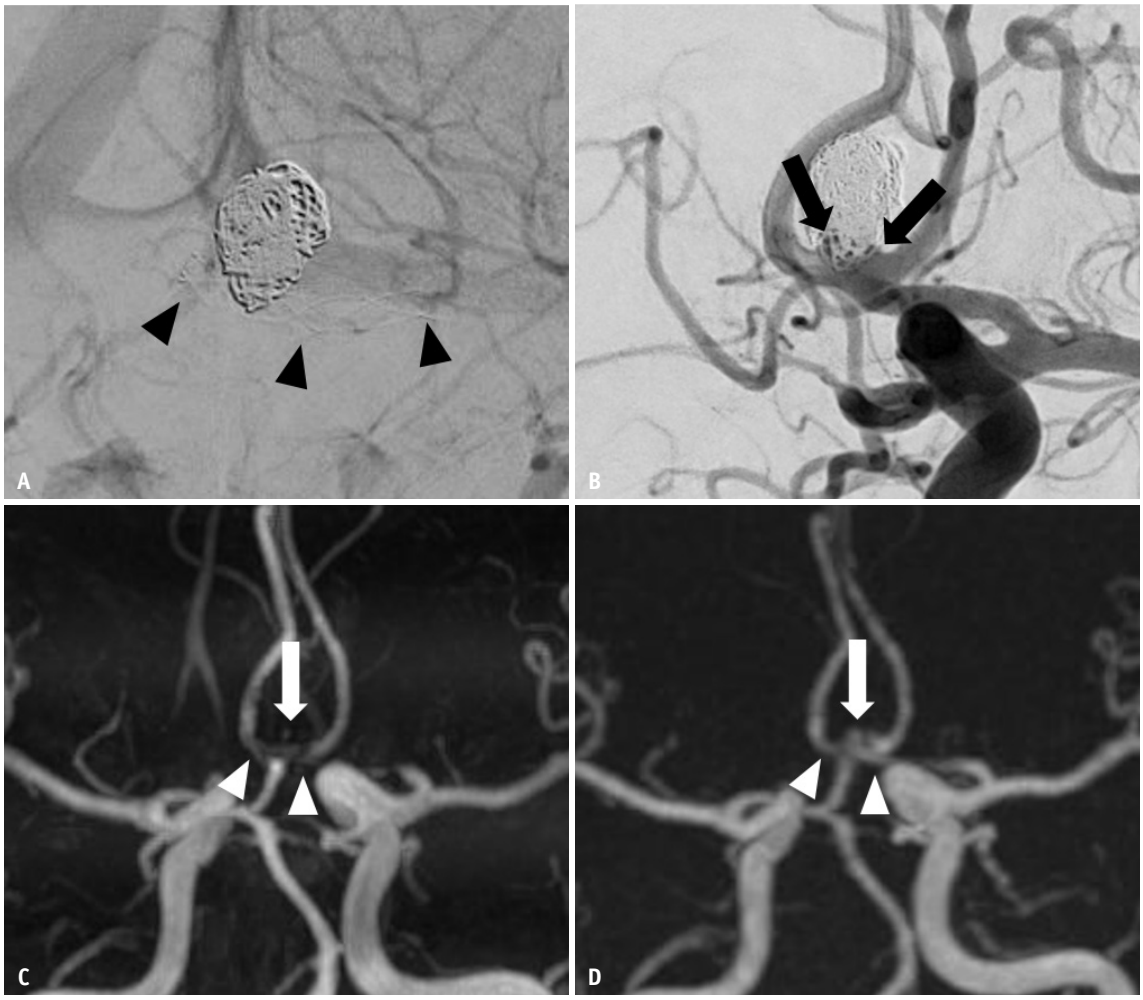

Fig. 3. Images of a 42-year-old male with a treated aneurysm in the anterior communicating artery.
A. Stent-assisted coil embolization was performed using an LVIS Jr stent. Arrowheads indicate implanted stent markers. **B.** Final angiography during the embolization procedure shows the neck remnant (arrows) of the aneurysm sac. **C.** Time-of-flight MRA shows acceptable visualization at the stented segment of the anterior cerebral artery (arrowheads), and the neck remnant is not depicted (arrow). **D.** Silent MRA shows excellent visualization at the stented segment (arrowheads), and the neck remnant is fully depicted (arrow). MRA = MR angiography

[30]. However, because the number of cases where the Solitaire AB stent was used was much smaller than that of other stents, this difference in sample size could also affect the results. Therefore, studies with a larger number of patients treated with Solitaire AB stents should be conducted in the near future to validate the significant results.

The self-expandable, single-wire braided nature of the LVIS Jr stent allows greater metal coverage of the blood vessel, compared with conventional open-cell and closed-cell stents. Because the metal quantity per unit blood vessel area is greater with the LVIS Jr stent, using TOF MRA to detect the neck remnants of aneurysms is considered more difficult due to susceptibility artifacts. However, the strut thickness of LVIS Jr stents (54 μm) is less than or similar to that of other stents (Enterprise, 94 μm; Solitaire AB, 61 μm; Neuroform Atlas, 55 μm). Hence, we assumed that the thickness of the LVIS Jr stent might affect the image quality and diagnostic accuracy of Silent MRA, which might be attributed to the reduction in susceptibility artifacts as a result of using a ZTE. Thus, Silent MRA might be useful for follow-up patients treated with LVIS Jr stents [4,30,31].

Silent MRA imaging takes 7 minutes 43 seconds, which is approximately 1.5 times longer than the 5 minutes 47 seconds required for TOF MRA. Owing to the long scanning duration, motion artifacts can be one of the disadvantages of Silent MRA. However, despite this disadvantage, Silent MRA provides benefits in flow visualization of the stented segment without contrast media or radiation exposure.

DSA is commonly considered a standard modality for

https://doi.org/10.3348/kjr.2021.0332

Korean Journal of Radiology
KJR

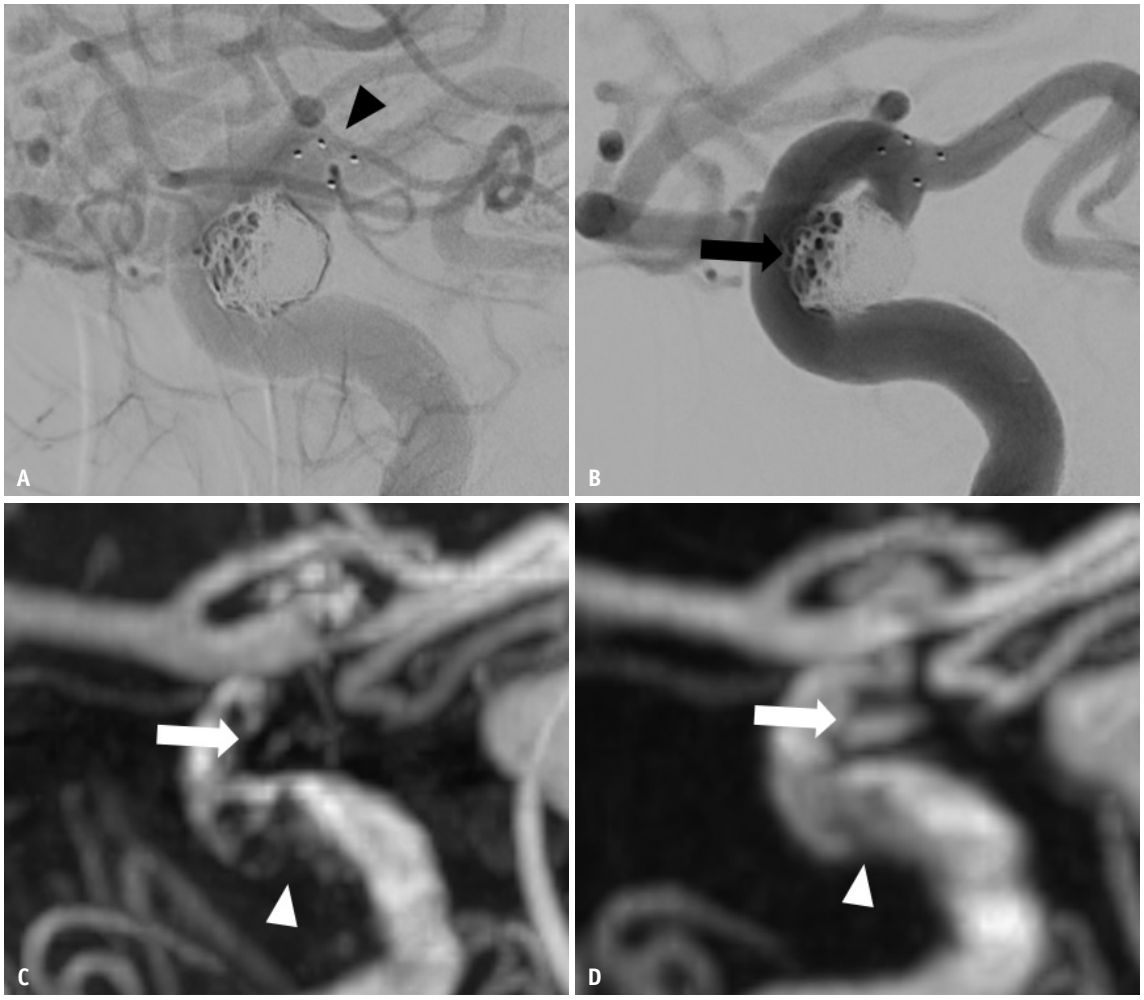

Fig. 4. Images of a 63-year-old female with a treated aneurysm in the right paraclinoid internal carotid artery.
A. Stent-assisted coil embolization was performed using a Solitaire AB stent. Arrowhead indicate implanted stent markers. **B.** Final angiography during the embolization procedure shows the neck remnant (arrow) of the aneurysm sac. **C.** Time-of-flight MRA shows poor visualization at the stented segment of the ICA (arrowhead), and the neck remnant is not depicted (arrow). **D.** Silent MRA shows excellent visualization at the stented segment (arrowhead), and the neck remnant is fully depicted (arrow). MRA = MR angiography

follow-up after stent-assisted coil embolization. However, this technique is invasive and carries risks associated with neurologic complications, contrast materials, and radiation exposure [3,6]. Therefore, as an alternative, CE MRA, a non-invasive technique, is used for follow-up imaging of stented aneurysms. However, this method has disadvantages, including gadolinium-induced nephrogenic systemic fibrosis and anaphylaxis [32]. Silent MRA can be used clinically as an imaging modality for the follow-up of aneurysms treated with stent-assisted coil embolization by compensating for these shortcomings.

This study has several limitations. First, there may be an information bias because TOF and Silent MRA were analyzed together without intervals, and the statistical power may have been jeopardized in the LVIS Jr and Solitaire AB stent groups because of the relatively small sample size. Second, Silent MRA has a longer scanning duration, which may cause motion artifacts. Third, TOF MRA and Silent MRA were used as follow-up imaging modalities 24 hours after treatment, meaning that our results cannot be extrapolated to long-term follow-up periods, something that can be addressed by future studies with longer follow-up periods. Fourth, we did not evaluate all types of stents currently used in stent-assisted coil embolization procedures. Finally, we were unable to compare Silent MRA with CE MRA, which is currently known to be useful as a follow-up imaging modality for stent-assisted coil embolization.

In conclusion, Silent MRA was superior to TOF MRA in the visualization of stented arteries and showed higher diagnostic accuracy for evaluating the status of aneurysm

 https://doi.org/10.3348/kjr.2021.0332

occlusion in patients who have undergone stent-assisted coil embolization, regardless of the aneurysm location and the type of stent used. The fact that patients are not exposed to radiation or contrast media is an advantage of Silent MRA. Silent MRA may, therefore, be useful for follow-up assessment after stent-assisted coil embolization.

Supplement

The Supplement is available with this article at https://doi.org/10.3348/kjr.2021.0332.

Availability of Data and Material

The datasets generated or analyzed during the study are available from the corresponding author on reasonable request.

Conflicts of Interest

The authors have no potential conflicts of interest to disclose.

Author Contributions

Conceptualization: Woo Sang Jung, You Na Kim, Jin Wook Choi. Data curation: Yong Cheol Lim, Jihye Song. Formal analysis: Ji Hyun Park. Investigation: Woo Sang Jung. Methodology: Woo Sang Jung. Project administration: Woo Sang Jung. Resources: Yong Cheol Lim, Jihye Song. Supervision: Woo Sang Jung. Writing—original draft: You Na Kim. Writing—review & editing: Woo Sang Jung.

ORCID iDs

You Na Kim
https://orcid.org/0000-0003-2771-2182
Jin Wook Choi
https://orcid.org/0000-0002-2396-4705
Yong Cheol Lim
https://orcid.org/0000-0002-5719-2483
Jihye Song
https://orcid.org/0000-0003-1949-6459
Ji Hyun Park
https://orcid.org/0000-0003-4182-7170
Woo Sang Jung
https://orcid.org/0000-0002-0727-3744

Funding Statement

An research grant was provided by Ajou University Hospital, 2020.

Acknowledgments

We would like to thank Editage (www.editage.co.kr) for English language editing.

REFERENCES

1. Molyneux AJ, Kerr RS, Yu LM, Clarke M, Sneade M, Yarnold JA, et al. International subarachnoid aneurysm trial (ISAT) of neurosurgical clipping versus endovascular coiling in 2143 patients with ruptured intracranial aneurysms: a randomised comparison of effects on survival, dependency, seizures, rebleeding, subgroups, and aneurysm occlusion. *Lancet* 2005;366:809-817
2. Mine B, Aljishi A, D'Harcour JB, Brisbois D, Collignon L, Lubicz B. Stent-assisted coiling of unruptured intracranial aneurysms: long-term follow-up in 164 patients with 183 aneurysms. *J Neuroradiol* 2014;41:322-328
3. Choi JW, Roh HG, Moon WJ, Chun YI, Kang CH. Optimization of MR parameters of 3D TOF-MRA for various intracranial stents at 3.0 T MRI. *Neurointervention* 2011;6:71-77
4. Cho YD, Kim KM, Lee WJ, Sohn CH, Kang HS, Kim JE, et al. Time-of-flight magnetic resonance angiography for follow-up of coil embolization with enterprise stent for intracranial aneurysm: usefulness of source images. *Korean J Radiol* 2014;15:161-168
5. Soize S, Gawlitza M, Raoult H, Pierot L. Imaging follow-up of intracranial aneurysms treated by endovascular means: why, when, and how? *Stroke* 2016;47:1407-1412
6. Kaufmann TJ, Huston J 3rd, Mandrekar JN, Schleck CD, Thielen KR, Kallmes DF. Complications of diagnostic cerebral angiography: evaluation of 19,826 consecutive patients. *Radiology* 2007;243:812-819
7. Irie R, Suzuki M, Yamamoto M, Takano N, Suga Y, Hori M, et al. Assessing blood flow in an intracranial stent: a feasibility study of MR angiography using a silent scan after stent-assisted coil embolization for anterior circulation aneurysms. *AJNR Am J Neuroradiol* 2015;36:967-970
8. Shang S, Ye J, Luo X, Qu J, Zhen Y, Wu J. Follow-up assessment of coiled intracranial aneurysms using zTE MRA as compared with TOF MRA: a preliminary image quality study. *Eur Radiol* 2017;27:4271-4280
9. Takano N, Suzuki M, Irie R, Yamamoto M, Teranishi K, Yatomi K, et al. Non-contrast-enhanced silent scan MR angiography of intracranial anterior circulation aneurysms treated with a low-profile visualized intraluminal support device. *AJNR Am J Neuroradiol* 2017;38:1610-1616
10. Heo YJ, Jeong HW, Baek JW, Kim ST, Jeong YG, Lee JY, et al. Pointwise encoding time reduction with radial acquisition with subtraction-based MRA during the follow-up of stent-assisted coil embolization of anterior circulation aneurysms. *AJNR Am J Neuroradiol* 2019;40:815-819
11. You SH, Kim B, Yang KS, Kim BK, Ryu J. Ultrashort echo time magnetic resonance angiography in follow-up of intracranial

aneurysms treated with endovascular coiling: comparison of time-of-flight, pointwise encoding time reduction with radial acquisition, and contrast-enhanced magnetic resonance angiography. *Neurosurgery* 2021;88:E179-E189
12. Ryu KH, Baek HJ, Moon JI, Choi BH, Park SE, Ha JY, et al. Usefulness of noncontrast-enhanced silent magnetic resonance angiography (MRA) for treated intracranial aneurysm follow-up in comparison with time-of-flight MRA. *Neurosurgery* 2020;87:220-228
13. Oishi H, Fujii T, Suzuki M, Takano N, Teranishi K, Yatomi K, et al. Usefulness of silent MR angiography for intracranial aneurysms treated with a flow-diverter device. *AJNR Am J Neuroradiol* 2019;40:808-814
14. Benitez RP, Silva MT, Klem J, Veznedaroglu E, Rosenwasser RH. Endovascular occlusion of wide-necked aneurysms with a new intracranial microstent (Neuroform) and detachable coils. *Neurosurgery* 2004;54:1359-1367; discussion 1368
15. Fiorella D, Albuquerque FC, Deshmukh VR, McDougall CG. Usefulness of the Neuroform stent for the treatment of cerebral aneurysms: results at initial (3-6-mo) follow-up. *Neurosurgery* 2005;56:1191-1201; discussion 1201-1202
16. Mocco J, Snyder KV, Albuquerque FC, Bendok BR, Alan S B, Carpenter JS, et al. Treatment of intracranial aneurysms with the Enterprise stent: a multicenter registry. *J Neurosurg* 2009;110:35-39
17. Higashida RT, Halbach VV, Dowd CF, Juravsky L, Meagher S. Initial clinical experience with a new self-expanding nitinol stent for the treatment of intracranial cerebral aneurysms: the Cordis Enterprise stent. *AJNR Am J Neuroradiol* 2005;26:1751-1756
18. Möhlenbruch M, Herweh C, Behrens L, Jestaedt L, Amiri H, Ringleb PA, et al. The LVIS Jr. microstent to assist coil embolization of wide-neck intracranial aneurysms: clinical study to assess safety and efficacy. *Neuroradiology* 2014;56:389-395
19. Behme D, Weber A, Kowoll A, Berlis A, Burke TH, Weber W. Low-profile Visualized Intraluminal Support device (LVIS Jr) as a novel tool in the treatment of wide-necked intracranial aneurysms: initial experience in 32 cases. *J Neurointerv Surg* 2015;7:281-285
20. Ge H, Lv X, Yang X, He H, Jin H, Li Y. LVIS stent versus enterprise stent for the treatment of unruptured intracranial aneurysms. *World Neurosurg* 2016;91:365-370
21. Klisch J, Eger C, Sychra V, Strasilla C, Basche S, Weber J. Stent-assisted coil embolization of posterior circulation aneurysms using solitaire ab: preliminary experience. *Neurosurgery* 2009;65:258-266
22. Klisch J, Clajus C, Sychra V, Eger C, Strasilla C, Rosahl S, et al. Coil embolization of anterior circulation aneurysms supported by the Solitaire AB Neurovascular Remodeling Device. *Neuroradiology* 2010;52:349-359
23. Mascitelli JR, Moyle H, Oermann EK, Polykarpou MF, Patel AA, Doshi AH, et al. An update to the Raymond–Roy occlusion classification of intracranial aneurysms treated with coil embolization. *J Neurointerv Surg* 2015;7:496-502
24. Viera AJ, Garrett JM. Understanding interobserver agreement: the kappa statistic. *Fam Med* 2005;37:360-363
25. DeLong ER, DeLong DM, Clarke-Pearson DL. Comparing the areas under two or more correlated receiver operating characteristic curves: a nonparametric approach. *Biometrics* 1988;44:837-845
26. van Holten J, Wielopolski P, Brück E, Pattynama PM, van Dijk LC. High flip angle imaging of metallic stents: implications for MR angiography and intraluminal signal interpretation. *Magn Reson Med* 2003;50:879-883
27. Lövblad KO, Yilmaz H, Chouiter A, San Millan Ruiz D, Abdo G, Bijlenga P, et al. Intracranial aneurysm stenting: follow-up with MR angiography. *J Magn Reson Imaging* 2006;24:418-422
28. Cho SB, Baek HJ, Ryu KH, Choi BH, Moon JI, Kim TB, et al. Clinical feasibility of zero TE skull MRI in patients with head trauma in comparison with CT: a single-center study. *AJNR Am J Neuroradiol* 2019;40:109-115
29. Takayama K, Taoka T, Nakagawa H, Myouchin K, Wada T, Sakamoto M, et al. Usefulness of contrast-enhanced magnetic resonance angiography for follow-up of coil embolization with the enterprise stent for cerebral aneurysms. *J Comput Assist Tomogr* 2011;35:568-572
30. Choi JW, Roh HG, Moon WJ, Kim NR, Moon SG, Kang CH, et al. Time-resolved 3D contrast-enhanced MRA on 3.0T: a non-invasive follow-up technique after stent-assisted coil embolization of the intracranial aneurysm. *Korean J Radiol* 2011;12:662-670
31. Wang Y, Truong TN, Yen C, Bilecen D, Watts R, Trost DW, et al. Quantitative evaluation of susceptibility and shielding effects of nitinol, platinum, cobalt-alloy, and stainless steel stents. *Magn Reson Med* 2003;49:972-976
32. Prince MR, Zhang H, Zou Z, Staron RB, Brill PW. Incidence of immediate gadolinium contrast media reactions. *AJR Am J Roentgenol* 2011;196:W138-W143

 https://doi.org/10.3348/kjr.2021.0332